Optics Communications 284 (2011) 5130–5134

Contents lists available at ScienceDirect

Optics Communications

journal homepage: www.elsevier.com/locate/optcom

Theoretical study of W-shaped optical fiber with a depression in core center by applying analytical transfer matrix method

JunAn Zhu, Lin Chen *, JiaMing Xu, ShiJie Li, YiMing Zhu **

School of Optics-Electrical and Computer Engineering, Engineering Research Center of Optical Instrument and System of Ministry of Education, Shanghai Key Lab of Modern Optical System, University of Shanghai for Science and Technology, No.516 Jungong Road, Shanghai 200093, China

ARTICLE INFO

Article history:
Received 26 November 2010
Received in revised form 5 July 2011
Accepted 5 July 2011
Available online 21 July 2011

Keywords:
Analytical transfer matrix method
Differential mode delay
W-shaped index profile

ABSTRACT

Analytical transfer matrix method (ATMM) is a method for calculating the propagation constant in weakly guiding optical fiber. By using ATMM, the optical fiber with a depression in the index profile center and a valley in the cladding layer is analyzed. Compared with Wentzel–Kramers–Brillouin (WKB) method, the simulation result of differential mode delay (DMD) by using ATMM fits well with the experimental results obtained by Takahashi. Based on ATMM, by increasing the depth of central depression in a W-shaped index fiber, the improvement of DMD is also discussed.

1. Introduction

In recent years, optics communication with dense-wavelength-division-multiplexing (DWDM) network has become the major communication mechanism for metropolitan wide-area networks and long-haul transmission system [1]. In order to acquire wide bandwidth and low dispersion, optical fibers are fabricated with various refractive index profiles, such as step form and graded form [2]. In particular, W-shaped refractive index profile in the silica-based multimode fiber (MMF) was proposed by Okoshi, Oyamada, and Okamoto [3,4], with an advantage in reducing model dispersion compared with graded index optical fiber. Lately, detail theoretical and experimental investigations taken by Ishigure et al. affirmed the advantage of W-shaped index profile [5–8]. For the theoretical analysis, WKB method, which is one of the well-known methods for solving one-dimensional Schrödinger equation in quantum theory and widely applied to optical waveguide because of its briefness, was used. However, the simulation results by using WKB method deviated from their experimental data. Although some modified WKB methods are developed, it still has some drawbacks [9], i.e., it is only accurate for a fiber with slowly changing index profile.

Analytical transfer matrix method (ATMM) originates from the matrix method to deal with the multi-layer waveguide [10–14]. The clear physical meaning and easy calculation for waveguide problems make ATMM suitable for the analysis of weakly guiding optical fibers with arbitrary refractive index profile [15]. As M.R. Shenoy has pointed out, matrix method can be applied to analyze the waveguide with more realistic continuous refractive index profiles compared to the depressed-inner-clad (DIC) fibers [10]. In this paper, ATMM is used to investigate DMD of the W-shaped optical fibers, which is caused by the modal dispersion. The calculated results of DMD fit well with the experimental results. Furthermore, the relation between DMD and depression in the center of index profile is also investigated.

2. Theory

2.1. The index profile

The index profile of a typical W-shaped optical fiber is shown by the following equation:

$$n = \begin{cases} n_1\sqrt{1-2\rho\Delta\left(\dfrac{r}{r_0}\right)^g} & 0 < r < r_0 \\ n_2 & r \geq r_0 \end{cases}, \tag{1}$$

where n_1 and n_2 are the refractive indices of core center and cladding layer, respectively. r_0 is the radius of core, and $\Delta = (n_1^2 - n_2^2)/(2n_1^2)$, which shows the relative index difference between the core center and the cladding layer. The parameters g is the index exponent and ρ is a parameter which determines the depth of the index valley. However, this equation cannot accurately show the measured index profile, because there is always a depression near the core center layer

* Correspondence to: L. Chen, Engineering Research Center of Optical Instrument and System, University of Shanghai for Science and Technology, No. 516 Jungong Road, Shanghai 200093, China.
** Correspondence to: Y.M. Zhu, Ministry of Education, University of Shanghai for Science and Technology, No. 516 Jungong Road, Shanghai 200093, China.
E-mail addresses: linchen@usst.edu.cn (L. Chen), ymzhu@usst.edu.cn (Y. Zhu).

0030-4018/$ – see front matter © 2011 Elsevier B.V. All rights reserved.
doi:10.1016/j.optcom.2011.07.005

in a typical W-shaped optical fiber and the index profile in cladding layer is not step-like function in real case [5–7]. Besides, when applying chemical-vapor-deposition (CVD) process, a depression also appears in the core center [16]. And all these depressions can affect the propagation properties of the optical fibers significantly, which deserves detail investigation. Ishigure et al. pointed out that their simulation by using this approximation as shown in Eq. (1) eventually led to a disagreement of DMD from their experimental results and the theoretical results [6]. Thus, in order to make our simulation more accurate, we fit this profile by the following equation

$$n = \begin{cases} -m_1(r-m_0)^2 + m_2 & \\ n_1\sqrt{1-2\rho\Delta\left(\dfrac{r}{r_0}\right)^g} & 0 \le r \le m_0 \\ & m_0 < r \le r_0 \\ \dfrac{m_3}{r+m_4} + m_5 & r > r_0 \end{cases}, \tag{2}$$

where m_0 is the boundary between the depression and the power-law part. The parameters in Eq. (2) are as follows.

$$m_0 = 57\ \mu\text{m},\ m_1 = 4.0012\times10^5\ \text{m}^{-2},\ m_2 = 1.51158,$$
$$m_3 = -0.18436\ \mu\text{m},\ m_4 = -184.10\ \mu\text{m},$$
$$m_5 = 1.5030,\ n_1 = 1.5117,\ \rho = 1.8,\ g = 4.1,\ r_0 = 200\ \mu\text{m}$$

The calculated index profile by using Eq. (2) is shown in Fig. 1, and our profile fits better with the experimental results than the simulation results obtained by Takahashi et al. [5].

2.2. Analytical transfer matrix method

A transverse field function used to describe the linear polarized (LP) mode for a certain optical fiber is like the following:

$$\frac{d^2F}{dr^2} + \frac{1}{r}\frac{dF}{dr} + \left[k_0^2n^2(r) - \beta^2 - \frac{l^2}{r^2}\right]F = 0. \tag{3}$$

For the easy calculation, a mathematical trick is introduced. We define an intermediate parameter

$$u(r) = \sqrt{r}F(r) \tag{4}$$

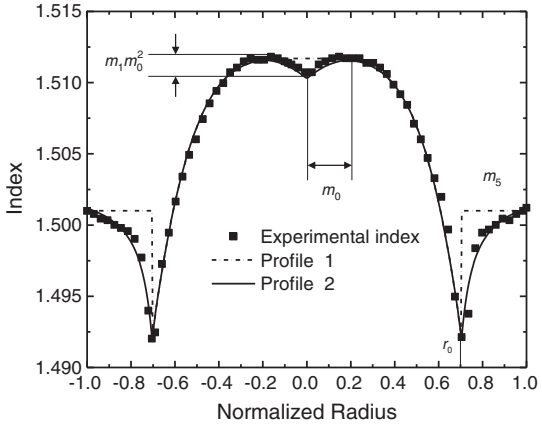

Fig. 1. The refractive index profile of the W-shaped optical fiber with a depression in the center. The square dots are measured results obtained by Takahashi et al. [1], while the dashed dotted line is plotted according to Eq. (1), and the solid line is plotted according to Eq. (2).

and the equivalent index n_{eq}

$$n_{eq}^2(r) = n^2(r) - \frac{l^2-\frac{1}{4}}{k_0^2r^2}. \tag{5}$$

Thus, we have

$$\frac{d^2u}{dr^2} + k_0^2\left[n_{eq}^2(r) - n_{eff}^2\right]u = 0, \tag{6}$$

where $n_{eff} = \beta/k_0$.

By substituting Eq. (2) into Eq. (5), we obtain the profiles of $n^2{}_{eq}$ of the W-shaped weakly guiding optical fiber which are shown in Fig. 2.

When $l>0$ (Fig. 2(a)), we truncate the profile at r_{min} and r_{max}. The field variations in (0, r_{min}) and (r_{max}, $+\infty$) cannot affect the calculation accuracy [15]. In the region (r_{low}, r_{high}), the electrical field shows an oscillatory behavior, while in the regions (r_{min}, r_{low}) and (r_{high}, r_{max}), the field shows an evanescent behavior. When $l=0$ (Fig. 2(b)), we truncate the profile at r_{low} and r_{max} similarly. The electrical field in (r_{low}, r_{high}) is oscillatory, while the field in (r_{high}, r_{max}) is evanescent. We divide the region (r_{min}, r_{low}), (r_{low}, r_{high}), and (r_{high}, r_{max}) into (low–min), (high–low) and (max–high) layers, respectively. (Note: 1. "min," "low," "high," and "max" are marked for r_{min}, r_{low}, r_{high}, r_{max}, respectively; 2. normally, 1000 layers in each region are enough, as the accuracy of n_{eff} can reach 1×10^{-7}, which is enough for the accuracy requirement in the following discussion. By using more layers, the improvement of accuracy is only in the order of 1×10^{-7}.)

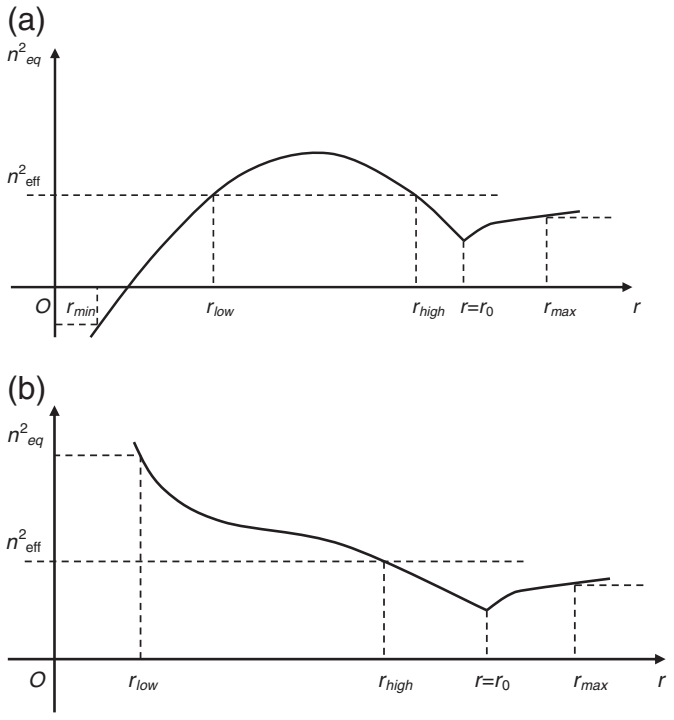

Fig. 2. The profile of the square of equivalent refractive index of W-shaped fiber $n^2{}_{eq}$. (a) When $l>0$, there are two intersections between $n^2{}_{eff}$ and $n^2{}_{eq}$. The profile is truncated at r_{min} and r_{max}; (b) when $l=0$, there is only one intersection between $n^2{}_{eff}$ and $n^2{}_{eq}$. The profile is truncated at r_{low} and r_{max}.

The transfer matrix of the jth layer in the region (r_{low}, r_{high}) is shown as follows [12–15]:

$$M_j = \begin{pmatrix} \cos(\kappa_j h_j) & -\frac{1}{\kappa_j}\sin(\kappa_j h_j) \\ \kappa_j \sin(\kappa_j h_i) & \cos(\kappa_j h_j) \end{pmatrix} j = \text{low}, \text{low}+1, \ldots, \text{high}-1, \text{high}, \tag{7}$$

where $\kappa_j = k_0\sqrt{n_{eq}^2(r_j) - n_{eff}^2}$ represents the transverse wave number, and h_j is the thickness of the jth layer.

Also, in the region (r_{min}, r_{low}) (this region does not exist when $l=0$) and (r_{high}, r_{max}), the transfer matrix of the ith layer is

$$M_i = \begin{pmatrix} \cosh(\alpha_i h_i) & -\frac{1}{\alpha_i}\sinh(\alpha_i h_i) \\ -\alpha_i \sinh(\alpha_i h_i) & \cosh(\alpha_i h_i) \end{pmatrix} \tag{8}$$

$$i = \text{min}, \text{min}+1, \ldots, \text{low}; \text{high}+1, \text{high}+2, \ldots, \text{max},$$

where $\alpha_i = k_0\sqrt{n_{eff}^2 - n_{eq}^2(r_i)}$ represents the evanescent behavior.

The recursion equation is as follows [17]:

$$\begin{pmatrix} u_{min} \\ u'_{min} \end{pmatrix} = \begin{cases} \prod_{i=\text{min}}^{\text{low}} M_i \prod_{j=\text{low}}^{\text{high}} M_j \prod_{i=\text{high}+1}^{\text{max}} M_i \begin{pmatrix} u_{max} \\ u'_{max} \end{pmatrix} & l > 0 \\ \prod_{j=\text{low}}^{\text{high}} M_j \prod_{i=\text{high}+1}^{\text{max}} M_i \begin{pmatrix} u_{max} \\ u'_{max} \end{pmatrix} & l = 0. \end{cases} \tag{9}$$

By simplifying Eq. (9), we have

$$\begin{pmatrix} u_s \\ u'_s \end{pmatrix} = M_s \begin{pmatrix} u_{s+1} \\ u'_{s+1} \end{pmatrix}, \; s = i \text{ or } j. \tag{10}$$

Now a parameter p is defined to express the field intensity,

$$p_s = \frac{u_s}{u'_s} = \frac{u(r_s)}{u'(r_s)}. \tag{11}$$

Thus, by simplifying Eq. (10), we obtain

$$p_j = \tan\left[\arctan\left(\frac{p_{j+1}}{p_j}\right) - \kappa_j h_j\right] \qquad j = \text{high}-1, \ldots, \text{low}+1 \tag{12}$$

and

$$p_i = \alpha_i \frac{\sinh(\alpha_i h_i) + \frac{p_{i-1}}{\alpha_i}\cosh(\alpha_i h_i)}{\cosh(\alpha_i h_i) + \frac{p_{i-1}}{\alpha_i}\sinh(\alpha_i h_i)}, \tag{13}$$

where

$$i = \begin{cases} \text{min}+1, \ldots, \text{low} \quad \text{high}+1, \ldots, \text{max} & l > 0 \\ \text{high}+1, \ldots, \text{max} & l = 0 \end{cases}.$$

Next, we rewrite Eq. (12) and get

$$\kappa_j h_j = q_j\pi + \arctan\left(\frac{p_j}{\kappa_j}\right) - \arctan\left(\frac{p_{j+1}}{\kappa_j}\right) \quad q_j = 0, 1, 2; j = \text{low}, \ldots, \text{high}-1. \tag{14}$$

Then, a typical eigen equation of the optical fiber [15] can be written as

$$\sum_{j=\text{low}}^{\text{high}-1} \kappa_j h_j + \Phi(s) = (m-1)\pi - \arctan\left(\frac{p_{\text{low}-1}}{\kappa_{\text{low}}}\right) - \arctan\left(\frac{p_{\text{high}}}{\kappa_{\text{high}-1}}\right), \tag{15}$$

where m is the radial order.

$$\Phi(s) = \sum_{j=\text{low}}^{\text{high}-2} \arctan\left[\left(\frac{p_{j+1}}{\kappa_{j+1}}\right) - \arctan\left(\frac{p_{j+1}}{\kappa_j}\right)\right]. \tag{16}$$

In the first layer, we can write

$$p_{\text{min}} = \begin{cases} \alpha(r_{min}) & l > 0 \\ \kappa(r_{\text{low}}) & l = 0 \end{cases}. \tag{17}$$

And in the last layer, the p_{max} can be written as,

$$p_{max} = \alpha(r_{max}). \tag{18}$$

Now, we already get the recursion equation (Eqs. (12) and (13)), together with the initial values of the recursion equation p_{min} and p_{max}. Thus, by substituting all these into Eq. (15), we can obtain the value of n_{eff} and β.

3. Simulation

To show the accuracy of ATMM, the normalized frequency V as the function of the normalized refractive index b of this particular optical fiber is calculated to make a comparison with the value which is obtained by finite element method (FEM). The parameter V and b are defined as:

$$V = k_0 n_1 r_0 \sqrt{2\Delta}, \tag{19}$$

$$b = \frac{n_{eff}^2 - n_2^2}{n_1^2 - n_2^2}. \tag{20}$$

The numerical results are shown in Fig. 3. From Fig. 3, we can see that the results of the ATMM are almost the same as those of the FEM. As a result, the accuracy of ATMM is proved.

In order to accurately analyze DMD of the W-shaped fiber, we use the index profile described by Eq. (2) instead of Eq. (1). By solving the eigen equation Eq. (15), we can get the effective index with a series of

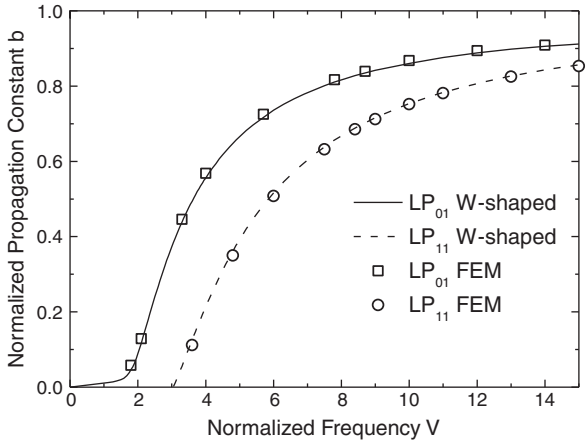

Fig. 3. V–b curve. The solid line is the V–b curve of LP_{01}, and the dashed line is the V–b curve of LP_{11}. The square dots and round dots are the exact value by FEM of LP_{01} and LP_{11}, respectively.

Table 1
n_{eff} with different LP modes (at wavelength 650 nm).

LP mode		No central depression	$m_1 = 4.0012 \times 10^5$	$m_1 = 3 \times 4.0012 \times 10^5$	$m_1 = 6 \times 4.0012 \times 10^5$
l	m	n_{eff}	n_{eff}	n_{eff}	n_{eff}
0	1	1.511687	1.511553	1.511547	1.511541
1	1	1.511673	1.511537	1.511519	1.511507
2	2	1.511607	1.511442	1.511399	1.511375
3	4	1.511462	1.511268	1.511184	1.511134
5	5	1.511329	1.511158	1.511062	1.511002
6	7	1.511138	1.510966	1.510842	1.510759
10	10	1.51071	1.510574	1.510446	1.510344
14	13	1.510228	1.510116	1.509998	1.50989
18	16	1.509701	1.509606	1.509502	1.509394
24	28	1.507875	1.507788	1.507679	1.507545
35	35	1.506178	1.506117	1.506043	1.505948
40	40	1.505079	1.505024	1.504959	1.504873
50	40	1.504359	1.504322	1.504283	1.504231
40	50	1.503501	1.503439	1.50336	1.503252
50	50	1.502736	1.502691	1.502639	1.502568
40	60	1.501844	1.501777	1.501687	1.501561
48	60	1.501199	1.501145	1.501078	1.500984

l and m (l and m are the subscripts of LP mode and represent azimuthal order and radial order, respectively), which is put in column 3 of Table 1. The numbers of effective index shown in column 4 and 5 will be discussed later.

The principal mode number is defined by $q = l + 2m$ [18], which means different LP mode can result in the same principal mode number as n_{eff} values of these LP modes are the same. The principal modes used to calculate DMDs are chosen according to Table 1.

The mode delay can be determined by the following equation [6]:

$$\tau = \frac{L}{c}\frac{k_0}{\beta}\frac{\int_{r_1}^{r_2}\frac{n^2 + nk_0\frac{dn}{dk_0}}{R}dr}{\int_{r_1}^{r_2}\frac{dr}{R}}, \tag{21}$$

with

$$R = \sqrt{n^2k_0^2 - \beta^2 - \frac{l^2}{r^2}}, \tag{22}$$

where n is the index profile in Eq. (2), c means the light velocity in vacuum, $L = 100$ m is the length of the fiber as presented in Ref. [5], r_1, r_2 are the roots of Eq. (22) at $R = 0$, and dn/dk_0 is determined by the relation between wavelength and refractive index of PMMA (polymethyl methacrylate) [19].

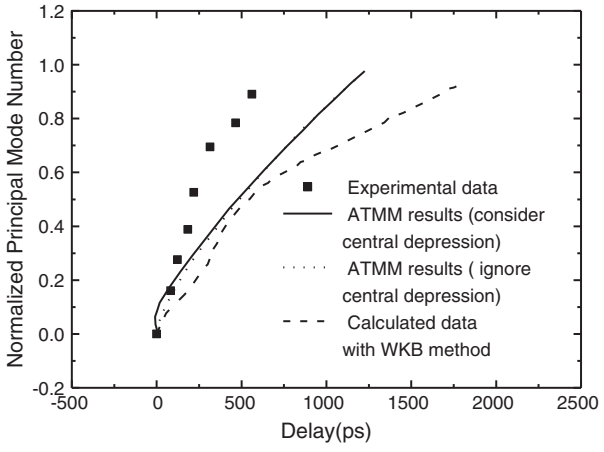

Fig. 4. The comparison of DMD data obtained by different methods. Square dots: measured DMD; solid line: calculated DMD with ATMM (ignore the central depression); dotted line: calculated DMD with ATMM (consider the central depression); dashed line: calculated DMD with WKB method by Takahashi et al. [5].

Substituting all the n_{eff} values shown in column 3 and 4 of Table 1 into Eq. (21), we obtain a series of mode delay values, and the DMD values can be obtained by subtracting the mode delay of the fundamental mode LP_{01}.

The normalized principal mode number is defined by q/Q, where Q is the max principal mode number [18]:

$$Q = \sqrt{\left(\frac{g}{g+2}\right)r_0^2k_0^2n_1^2\Delta}. \tag{23}$$

The simulation results calculated by ATMM, the simulation results calculated by Takahashi et al. [5], and the experimental data obtained by Takahashi et al. [5] are shown in Fig. 4. The DMDs of some principal modes are presented in Table 2 to make a comparison between the accuracy of ATMM and WKB method, in which the exact values are the experimental results. From Fig. 4, we can see that ATMM results are closer to the experimental result compared to WKB method. The difference between ATMM and experimental result is caused by the slightly difference in the quadratic part of the index profile. We cannot fit the index profile of an optical fiber perfectly. Furthermore, there are always some undulations in the profile which we have to ignore. In Fig. 4, there is a large difference between the result of WKB and measured DMD in the high-order modes, as the higher order modes carry more energy in their evanescent field, which is strongly affected by the index profile at the core-cladding boundary, than those in the lower order modes. Thus, the group delay of the high-order modes shows great difference to the experimental result [7].

The calculated DMD of the fiber with no central depression is slightly different to the one with depression in the core center, and

Table 2
DMDs of exact results [1], ATMM results and WKB results.

Principal mode	Exact	ATMM	WKB
q	DMD (ps)		
0.01163	0	0	0
0.1603	82.2	0.6	3.6
0.27608	123.3	192.1	302.2
0.388	183.6	300.6	384.2
0.52543	219.2	513.6	571.3
0.69464	315.1	763.3	1043.7
0.7837	465.8	904.3	1327.1
0.89057	561.6	1078.6	1664.1

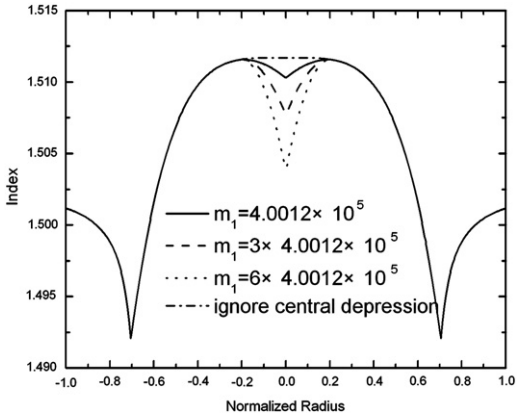

Fig. 5. Refractive index profile with different depression depths.

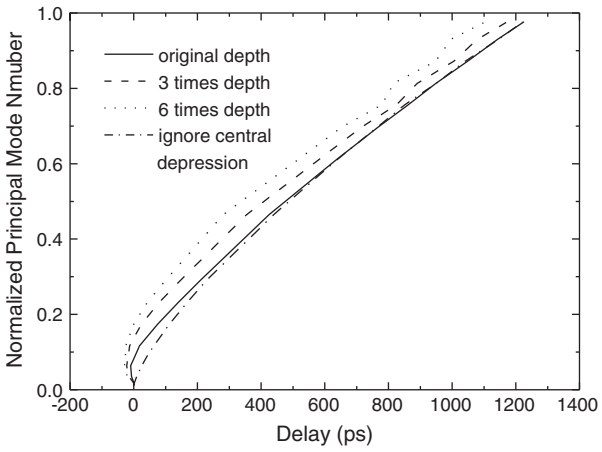

Fig. 6. DMD with different depths of depression calculated by ATMM. Dashed dotted line: DMD in the fiber without central depression; solid line: DMD in the fiber with original depression; dashed line: DMD with the depression of 3 times depth; dotted line: DMD with the depression of 6 times depth.

both of them are closer to the experimental results compared to the one obtained by WKB method.

Furthermore, we also research the depth of the depression in core center in order to investigate detail property of W-shaped optical fiber. In Eq. (2), we defined a parameter m_1 to describe the profile in the depression region. The depth of the depression in the center increases with the increase of m_1. In order to give a brief illustration of the effect on DMD caused by the change of m_1, we calculate the values of n_{eff} with different m_1, i.e., $m_1 = 4.0012\times10^5$ (original depth), $3\times4.0012\times10^5$ (3 times depth), and $6\times4.0012\times10^5$ (6 times depth), and these refractive index profiles are shown in Fig. 5. The values of n_{eff} are shown in column 4 and 5 of Table 1. Then, by using the values of n_{eff}, we can get the values of DMD (Fig. 6).

From Fig. 6, we can see that when increasing the depression depth in the core center, the delay time decreases. It is proved by Ishigure et al. that the group delay difference between the highest and lowest order modes in W-shaped fiber is much smaller than that in the graded index fiber, which is caused by the modal dispersion compensation effect from the refractive index valley [6]. In Fig. 6, we can see the central depression also contributes to the modal dispersion compensation effect. Furthermore, as the energy of low order modes concentrates on the core center, the change of the depth of the depression leads to the change of group delay, especially in the low order modes. With short group delay time, the velocity difference of each mode propagating along the fiber is slight, which implies that the dispersion effect and the loss of field energy are reduced. Deep depression in the central of refractive index profile helps to decrease the modal dispersion effect. It leads to a long relay distance when the W-shaped fiber is applied to communication networks.

4. Conclusion

In this paper, the values of DMD in a typical W-shaped fiber with the different central depression are discussed. Based on the discussion above, ATMM can be used to analyze the weakly guiding fiber with arbitrary index profile, and the results calculated by ATMM theory show better fitting with the experimental results presented by Takahashi et al. [5] than by WKB method. Furthermore, we also suggest that with the increasing depth of original depression in the center of index profile, the value of DMD is reduced, which also leads to good communication quality.

Acknowledgment

The authors would thank Dr. Zheng Liang for useful help. This work was partly supported by the Research Fund for “Chen Guang” project supported by Shanghai Municipal Education Commission and Shanghai Education Development Foundation (grant no. 09CG49), Shanghai Committee of Science and Technology (grant no. 11ZR1425000, 09QA1404200), the Nano-tech Foundation of Shanghai Committee of Science and Technology (grant no. 0952nm02400), The National Undergraduates' Innovation Experiment Program (091025213), Ph.D. Programs Foundation of Ministry of Education of China (20093120120007), and National Natural Science Foundation of China (61007059), and Shanghai PuJiang Program from Science and Technology Commission of Shanghai (09PJ1407800).

Reference

[1] I.B. Djordjevic, S. Sankaranarayanan, B.V. Vasic, J. Lightwave Technol. 22 (3) (Mar. 2004) 695.
[2] R.L. Lachance, P.-A. Bélanger, J. Lightwave Technol. 9 (11) (Nov. 1991) 1425.
[3] K. Okamoto, T. Okoshi, IEEE Trans. Microwave Theory Tech. 25 (3) (Mar. 1977) 213.
[4] K. Oyamada, T. Okoshi, IEEE Trans. Microwave Theory Tech. 28 (10) (Oct. 1980) 1113.
[5] K. Takahashi, T. Ishigure, Y. Koike, J. Lightwave Technol. 24 (7) (Jul. 2006) 2867.
[6] T. Ishigure, H. Endo, K. Ohdoko, K. Takahashi, Y. Koike, J. Lightwave Technol. 23 (4) (Apr. 2005) 1754.
[7] T. Ishigure, H. Endo, K. Ohdoko, Y. Koike, IEEE Photonics Technol. Lett. 16 (9) (Aug. 2004) 2081.
[8] T. Yamashita, M. Kagami, J. Lightwave Technol. 23 (8) (Aug. 2005) 2542.
[9] A. Gedeon, Opt. Commun. 12 (3) (Nov. 1974) 329.
[10] M.R. Shenoy, K. Thyagarajan, A.K. Ghatak, J. Lightwave Technol. 6 (8) (Aug. 1988) 1285.
[11] Z. Cao, C. Hu, G. Jin, J. Opt. Soc. Am. B 8 (12) (Dec. 1991) 2519.
[12] Z.Q. Cao, Y. Jiang, Q.S. Shen, X.M. Dou, Y.L. Chen, J. Opt. Soc. Am. A 16 (1999) 2209.
[13] Z.Q. Cao, Q. Liu, Q.S. Shen, X.M. Dou, Y.L. Chen, Y. Ozaki, Phys. Rev. A 63 (2001) 054103.
[14] Z.Q. Cao, Q. Liu, Y. Jiang, Q.S. Shen, X.M. Dou, Y. Ozaki, J. Opt. Soc. Am. A 18 (2001) 2161.
[15] Z. Liang, Z. Cao, Q. Shen, X. Deng, J. Lightwave Technol. 23 (2) (Feb. 2005) 849.
[16] A.K. Ghatak, R. Srivastava, Appl. Opt. 22 (11) (1983) 1763.
[17] Q. Liu, Z. Cao, Q. Shen, X. Dou, Y. Chen, Opt. Quantum. Electron. 33 (6) (2001) 675.
[18] I. Takaaki, K. Mariko, K. Yasuhiro, J. Lightwave Technol. 18 (7) (2000) 959.
[19] K. Liu, R. Yu, Acta Photonica Sin. 31 (7) (2002) 819.